Experimental demonstration of robustness and accuracy of a DLI-based OSNR monitor under changes in the transmitter and link for different modulation formats and baud rates

Ahmed Almaiman,[1,*] Mohammad Reza Chitgarha,[1] Wajih Daab,[1] Morteza Ziyadi,[1] Amirhossein Mohajerin-Ariaei,[1] Salman Khaleghi,[1] Moshe Willner,[1] Vijay Vusirikala,[2] Xiaoxue Zhao,[2] Dan Kilper,[3] Loukas Paraschis,[4] Atiyah Ahsan,[5] Michael Wang,[5] Keren Bergman,[5] Moshe Tur,[6] Joseph D. Touch,[7] Alan E. Willner[1]

[1] *Ming Hsieh Department of Electrical Engineering, University of Southern California, Los Angeles, CA 90089, USA*
[2] *Google Inc., 1600 Amphitheatre Parkway, Mountain View, CA 94043, USA*
[3] *College of Optical Sciences, University of Arizona, Tucson, AZ, USA*
[4] *Optical Networking, Advanced Technology and Planning, Cisco Systems, Inc.*
[5] *Lightwave Research Lab, Department of Electrical Engineering, Columbia University, New York, NY*
[6] *School of Electrical Engineering, Tel Aviv University, Ramat Aviv 69978, Israel*
[7] *Information Sciences Institute, University of Southern California, 4676 Admiralty Way, Marina del Rey, CA, 90292, USA*
**Corresponding author: almaiman@usc.edu*

Received Month X, XXXX; revised Month X, XXXX; accepted Month X, XXXX; posted Month X, XXXX (Doc. ID XXXXX); published Month X, XXXX

We experimentally studied the performance of a delay-line interferometer-based optical signal-to-noise ratio (OSNR) monitor, that is pre-calibrated in optimal conditions for 25 Gbaud pol-muxed quadrature-amplitude-modulation (QAM) signals, when unpredicted changes outside the monitor occurred either in the transmitter or the link.

OCIS Codes: (060.2330) Fiber Optics Communications, (060.2360) Fiber Optics Links And Subsystems, (060.4257) Networks, Network Survivability.
http://dx.doi.org/10.1364/OL.99.099999

Optical performance monitoring has gained much interest for potentially enabling efficient operation and management of dynamic optical networks. High-speed networks are subject to optical signal degradation, partially due to the amplified spontaneous emission (ASE) noise originating from erbium-doped fiber amplifiers (EDFA). Therefore, measuring the OSNR can be key in diagnosing the health of an optical communication system. Knowledge of the OSNR can help to: (i) identify failures and repair the network, (ii) re-route traffic, and (iii) allocate resources [1,2].

The OSNR is traditionally determined by interpolating the in-band noise based on out-of-band noise measurements, which is approximate and is difficult to realize accurately in the presence of switches due to out-of-band filtering effects. Other OSNR monitoring approaches may utilize polarization [3], or digital signal processing [4-6]. The former approach might be difficult to use with polarization multiplexed (pol-muxed [PM-]) signals, whereas the latter tends to require a full receiver for implementation.

In general, an OSNR monitor should be cost effective, robust, and independent of both the modulation format and bit rate. A delay-line interferometer (DLI) with quarter-bit delay-based OSNR monitoring was reported and has shown relative polarization independence and <0.5 dB measurement error [7,8]. Operating guidelines, crosstalk dependencies, structure, and network decision support were explored in [9-15]. This DLI-based OSNR monitor is based on the principle of distinguishing the relative coherence between the signal and the noise. It measures the OSNR based on the relative output power at the constructive and destructive ports of a DLI, such that the signal experiences coherent interference and the noise does not. In general, this approach tends to require some *a-priori* knowledge of the initial conditions of the DLI-based monitor parameters, i.e., calibration..

In [16], the dependence of the calibration on the extinction ratio was first reported for direct detection-based systems. However, the precision of a fixed single-DLI monitor with changing system conditions has not been investigated, which may not remain robust: (a) if the signal encounters transmitter drift or a change in its parameters, (b) if the network operator propagates a different data signal in the link or replaces the transmitter unit, and (c) if the baud rate or modulation format of the data channel is varied.

In this letter, we experimentally examine the monitor accuracy when the initially measured conditions of the DLI-based monitor for a 25 Gbaud pol-muxed quadrature-phase-shift-keying (QPSK) signal are kept fixed without updating (*e.g.,* pre-calibrated) in the presence of various systems changes by modifying the transmitter and link parameters. The error in the OSNR reading as compared to an actual OSNR in the range of 10 to 20 dB remained <0.5 dB for changing modulation formats, transmitter modulator phase bias drift up to 32% of the half-wave voltage (V_π), and the modulator bias drifting within 20% of

V_π. However, errors exceeded 0.5 dB when the baud rate was tuned to 24 and 26 Gbaud without re-adjusting the DLI parameters used for the OSNR calculation.

The fundamental block for the DLI monitor consists of a band-pass filter (BPF) to select the desired channel and limit the noise, a DLI to split the incoming power into two different paths, power measurement units, and a simple processor to calculate the OSNR. When the DLI phase is at the null point, a small amount of modulated coherent signal power will appear at the DLI destructive port, while most of the power will appear at the constructive port. Thus, the ratio of the constructive power to the destructive power is much greater than one. However, when noncoherent noise arrives at the DLI, its power will split nearly equally, resulting in a power split ratio close to unity.

Because filters are linear systems, with the previous knowledge of distribution factors (*i.e.*, calibration) of the two extreme cases—(i) noise-free signal (α) and (ii) the noise itself (β)—it is possible to represent the OSNR as a function of the distribution factor of the channel under test (δ) [17]. OSNR measurement thus depends on the matching between calibration factors and the channel being tested. This is shown in Eqs. (1) and (2) where $P_{Const,Signal}$, $P_{Const,Noise}$, $P_{Const,Channel}$, $P_{Dest,Signal}$, $P_{Dest,Noise}$, and $P_{Dest,Channel}$ are the powers for signal, noise, and the channel under examination at the constructive and destructive ports, respectively. We also define *NEB* as the noise equivalent bandwidth of the BPF.

$$\alpha = \frac{P_{Const,Signal}}{P_{Dest,Signal}} \quad , \quad \beta = \frac{P_{Const,Noise}}{P_{Dest,Noise}} \quad , \quad \delta = \frac{P_{Const,Channel}}{P_{Dest,Channel}} \tag{1}$$

$$OSNR\ (dB) \triangleq 10log_{10}\left(\frac{(\alpha+1)\times(\delta-\beta)}{(\beta+1)\times(\alpha-\delta)} \times \frac{NEB}{0.1\ nm}\right) \tag{2}$$

As depicted in Fig.1, we initially calibrated the monitor with its signal and noise distribution factors α and β under optimal conditions, defined as having flat spectrum ASE noise and a perfectly biased signal. We then varied the (i) phase bias, (ii) modulator bias, (iii) baud rate, (iv) modulation format, (v) wavelength, and (vi) link and measured the induced error in the OSNR reading. The changing conditions (i–vi) were emulated through tuning the transmitter parameters, and the cascaded structure of amplifiers represents longer links.

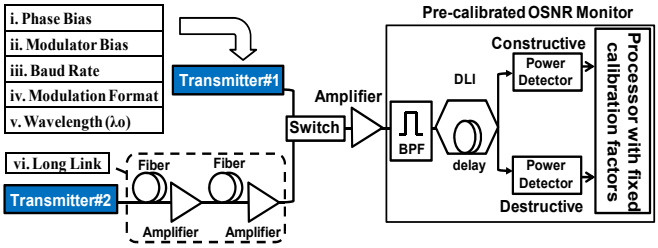

Fig.1. The concept of using a pre-calibrated DLI-based OSNR monitor under changing conditions.

We also related drifting bias scenarios to error vector magnitude (*EVM*) in Eq. (3) to evaluate the back-to-back modulated signal at the transmitter, as in [18], where x_j is the detected symbol, s_j is the closest member of the symbol alphabet, and N is 4096 in our coherent receiver.

$$EVM = 100\% \cdot \sqrt{\frac{\frac{1}{N}\sum_{j=1}^{N}|s_j - x_j|^2}{\frac{1}{N}\sum_{j=1}^{N}|s_j|^2}} \tag{3}$$

The experimental setup is depicted in Fig.2. An in-phase/quadrature (I/Q) modulator was driven by 2^{31}-1 pseudo-random bit sequences (PRBS) with a variable clock to modulate a wavelength tunable continuous-wave (CW) laser. The modulator could be controlled to transmit either a binary-phase-shift-keying (BPSK) or QPSK signal. The clock can also be varied to generate different baud rates (10 to 30 Gbaud). The I/Q modulator has an automatic bias control circuit (ABC) to optimize the inner Mach-Zehnder modulators (MZM_I and MZM_Q) bias voltages (V_I and V_Q) and to keep them at the null point. Moreover, the phase bias voltage (V_{Phase}) was optimized to realize a perfect QPSK constellation (ϕ=90°). In this experiment, the measured modulator's V_π was 9.2 V. The modulator output was then sent to a higher-order QAM emulator to generate a 16-QAM signal. A single polarized signal was amplified and then split, delayed, and combined in a polarization beam splitter (PBS) to generate the pol-muxed signal. The signal at the transmitter was tapped to measure the back-to-back *EVM* and capture the constellation at the coherent receiver.

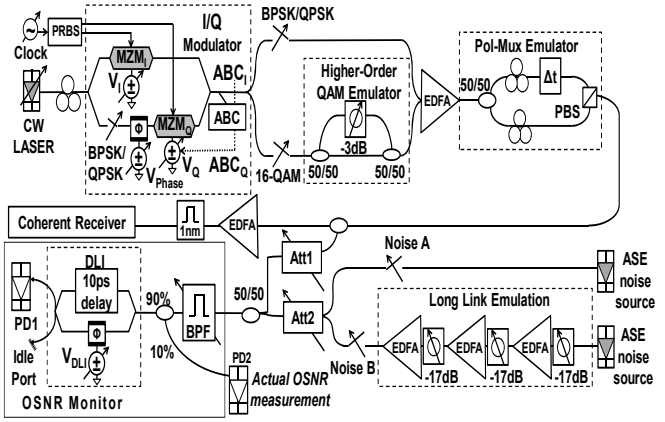

Fig.2. Pre-calibrated OSNR monitor experimental setup with unpredicted changing scenarios in the transmitter and link.

Noise was generated either by using an ASE source, for Noise A, or through three consecutive EDFAs to emulate the noise accumulated through long links in Noise B. Both signal and noise were combined in a 50/50 coupler through variable attenuators for power adjustment, and then sent to the DLI-based OSNR monitor. The monitor has a 0.3 nm BPF connected to a polarization-insensitive DLI with a 100 GHz free spectral range (10 ps) and low-speed photodiode PD1 (*i.e.*, power detector) with 0.5% accuracy and 0.01 dB resolution. Using a configuration similar to that in [7], only one of the output ports was connected to a low-speed photodiode to record the constructive and destructive powers when sweeping the DLI phase voltage (V_{DLI}) over a full cycle of $2V_\pi$.

We initialized the OSNR monitor by measuring the calibration factors α and β for the optimal 100 Gb/s 25 Gbaud PM-QPSK signal at 1552.52 nm (193.1 THz) impaired with Noise A. Both α and β were measured when attenuators blocked either the noise or the signal,

respectively. The actual OSNR was measured at photodiode PD2 using the 10% tap after the BPF.

First, we studied the impact of imperfect phase bias adjustment (Fig.3). Figure 3(a) shows that the back-to-back *EVM* reached 48.75% when the normalized phase bias voltage drift ($V_{Phase,Drift}$) defined in Eq. (4) was at 32%, where $V_{Phase,optimal}$ is the optimal voltage for ϕ=90°. However, the OSNR monitor measurement showed independence of the signal phase bias and could still successfully read the OSNR within 0.5 dB of error. Fig.3(c) shows the back-to-back constellations at the different *EVM*s in the experiment. According to [19], this independence can be explained by the fact that modulator phase changes do not change the power detected at power meters.

$$V_{Phase,Drift} = \frac{V_{Phase} - V_{Phase,optimal}}{V_{\pi}} \quad (4)$$

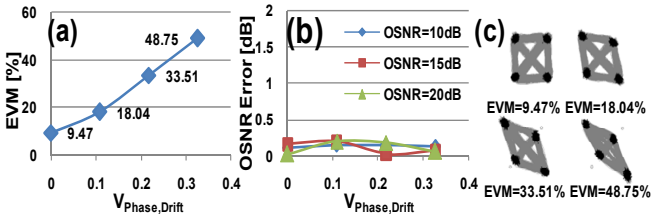

Fig.3. Experimentally measured back-to-back *EVM* and OSNR reading error for the noise-impaired signal under imperfect phase bias for the 100 Gb/s PM-QPSK signal in (a) and (b), respectively. (c) Captured constellations corresponding to *EVM*s.

We then tuned the bias on the inner MZMs and defined the normalized drifting on these inner modulators, $V_{I,Drift}$ and $V_{Q,Drift}$ in Eq. (5) where $V_{I,null}$, and $V_{Q,null}$ are the optimal null-point bias voltages.

$$V_{I,Drift} = \frac{V_I - V_{I,null}}{V_{\pi}} \quad , \quad V_{Q,Drift} = \frac{V_Q - V_{Q,null}}{V_{\pi}} \quad (5)$$

We first measured the error when the I-modulator was connected to the automatic bias control ($V_{I,Drift}$=0) while the Q-modulator was manually changed from its optimal state ($V_{Q,Drift}\neq$0). Figure 4(a) and (b) show the impact of $V_{Q,Drift}$ degradation from 0 to 54%. The 20 dB OSNR case showed a 0.5 dB error after 24% of $V_{Q,Drift}$ degradation corresponding to 1 percentage degradation in *EVM*, and the error reached 1.5 dB at the $V_{Q,Drift}$ of 54%. The 0.5 dB error occurred for the 15 dB OSNR case at 45% of $V_{Q,Drift}$ corresponding to 3 percentages degradation compared to the initial *EVM*. The recorded constellations of this experiment are shown in Fig.4(c).

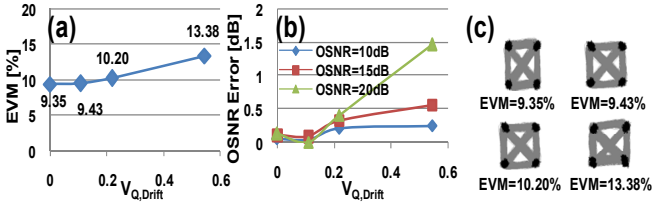

Fig.4. Experimentally measured (a) back-to-back *EVM* and (b) OSNR error against voltage drifting on a single MZM for a 100 Gb/s PM-QPSK transmitter. (c) Captured constellations corresponding to *EVM*s in the coherent receiver.

For further analysis, random drifting was applied to both inner modulators (I and Q), as shown in Fig.5. Results are plotted against the normalized root mean square voltage drifting ($V_{RMS,Drift}$) calculated as shown in Eq. (6). The measured back-to-back *EVM* at various $V_{RMS,Drift}$ points is shown in Fig.5(a). Figure 5(b) shows that OSNR measurements could encounter 1 dB of error in the 20–40% range of $V_{RMS,Drift}$ and up to 1.7 dB of error when drifting higher than 40% of $V_{RMS,Drift}$ for the high OSNR case (OSNR=20 dB) occurs. Even so, state-of-the-art bias controllers allow negligible drifting under normal conditions [20]. Figure 5(c), presents the constellations of *EVM*s and their corresponding $V_{I,Drift}$ and $V_{Q,Drift}$.

$$V_{RMS,Drift} = \sqrt{V_{I,Drift}^2 + V_{Q,Drift}^2} \quad (6)$$

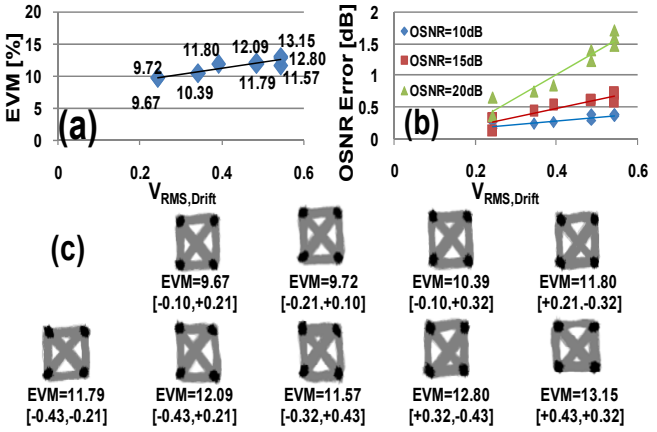

Fig.5. (a) Back-to-back *EVM* and (b) OSNR error caused by random drifting on both I/Q modulator inner MZMs. (c) Constellations at various *EVM*s and their applied drifting voltages [$V_{I,Drift}$,$V_{Q,Drift}$].

Figure 6 shows the impact of changing the baud rate and modulation format. The OSNR measurement error when varying only the baud rate and using the pre-calibration of the 25 Gbaud PM-QPSK signal is depicted in Fig.6(a). A 1-Gbaud change in the baud rate caused more than 0.5 dB error for 15 and 20 dB OSNR cases. This suggests that the OSNR monitor does not tolerate such changes without *a-priori* knowledge and re-calibration. This is supported by Fig.6(b), where PM-BPSK, PM-QPSK, and PM-16-QAM signal calibration factors are plotted against the applied baud rate and they change from 43 to 13 in the range of 10–30 Gbaud which means calibration is baud rate dependent

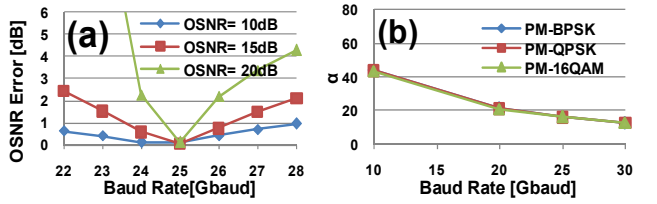

Fig.6. Experimentally measured (a) PM-QPSK signal OSNR error reading when tuning the baud rate while utilizing the 25 Gbaud pre-calibration factors, and (b) signal distribution factors at different baud rates for PM-signals (BPSK, QPSK, and 16-QAM).

Similarities in these modulation formats' signal distribution factors further suggest that signals that are constructed by the coherent addition of the same basic signal preserve the same signal distribution factor over DLI ports (*i.e.*, QPSK and 16-QAM signals represent the

coherent addition of BPSK signals [21]). At the baud rates in Fig.6(b), the PM-QPSK calibration was applied to both PM-BPSK and PM-16-QAM for OSNR measurement and the error did not exceed 0.5 dB at 10, 15, and 20 dB OSNRs. In other words, it is only necessary to pre-calibrate for one modulation format at each planned baud rate to operate with less than 0.5 dB error. If 16-QAM signal is generated utilizing an optical I/Q modulator driven by 4-level electrical signals, it might be needed to re-calibrate again for that particular transmission signal.

The monitor's performance under the changing wavelength is depicted in Fig.7. This figure shows the maximum recorded error when we changed the wavelength and the BPF to a different ITU grid channel within the range of 1548–1561 nm (specifically: 1548.34, 1552.93, 1554.54, 1556.55, and 1560.61 nm). We tested applying the pre-calibration factors of the middle point (1554.54 nm) on all other channels without re-calibration, and tested updating the calibration in the monitor at each wavelength before OSNR measurement. In the first test, the maximum measured error was >0.5 dB at around 0.7 dB for the 20 dB OSNR case. This error might be due to the filter spectral profile dependence on the wavelength. However, the low and medium OSNRs' (10 and 15 dB) maximum errors remained within the 0.5 dB range. Therefore, for applications with tight constrains on the OSNR reading error at higher OSNRs, keeping calibration record for each wavelength is necessary.

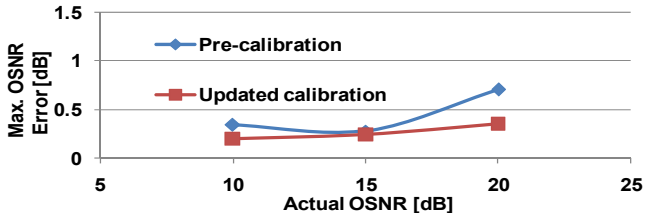

Fig.7. The effect of changing the wavelength of a 100 Gb/s PM-QPSK signal and the maximum recorded error when (a) 1554.54 nm calibration was used as a global pre-calibration, and (b) updating the calibration was conducted at each wavelength.

The study of the monitor's performance under the condition of changing the link is shown in Fig.8. The ASE spectrums for the initial and re-routed noises (Noise A and B, respectively) are shown in Fig.8(a). Figure 8(b) indicates that OSNR error stayed in the range of <0.5 dB when noise propagated through a long link scenario for 1552.52 nm PM-QPSK or PM-16-QAM signals at 25 Gbaud.

Our results focus mainly on experimental measurements. However, future simulation and theoretical analysis of the relationship between various impairments and OSNR measurement errors might provide insight into a more robust monitoring solution. For example, a network may be designed to operate under different pre-defined operating parameters. Subsequently, a network controller may potentially utilize the feedback from other elements in other parts of the network to help identify the impairments and correct the OSNR monitoring errors.

The authors acknowledge the support of Google and the NSF CIAN.

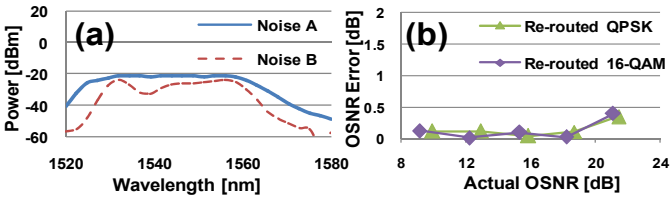

Fig.8. (a) ASE noise profiles. (b) OSNR error for the re-routed noise scenario.

References

1. D. C. Kilper, R. Bach, D. J. Blumenthal, D. Einstein, T. Landolsi, L. Ostar, M. Preiss, and A. E. Willner, J. Lightwave Technol. **22**, 294 (2004).
2. Z. Pan, C. Yu, and A. E. Willner, Opt. Fiber Technol. **16**, 20 (2010).
3. J. H. Lee, H. Y. Choi, S. K. Shin, and Y. C. Chung, J. Lightwave Technol. **24**, 4162 (2006).
4. D. J. Ives, B. C. Thomsen, R. Maher, and S. J. Savory, Opt. Express **19**, B661 (2011).
5. J. C. Li, T. B. Anderson, and T. J. Morgan, IEEE Photon. Technol. Lett. **23**, 983 (2011).
6. D. Zhao, L. Xi, X. Tang, W. Zhang, Y. Qiao, and X. Zhang, IEEE Photon. J. **6**, 7902009 (2014).
7. X. Liu, Y.-H. Kao, S. Chandrasekhar, I. Kang, S. Cabot, and L. L. Buhl, IEEE Photon. Technol. Lett. **19**, 1172 (2007).
8. Y. K. Lizé, J.-Y. Yang, L. Christen, X. Wu, S. Nuccio, T. Wu, A. E. Willner, R. Kashyap, and F. Séguin, in *Optical Fiber Communication Conference*, (Optical Society of America, 2007), paper OThN2.
9. M. R. Chitgarha, S. Khaleghi, W. Daab, A. Almaiman, M. Ziyadi, A. Mohajerin-Ariaei, D. Rogawski, M. Tur, J. D. Touch, V. Vusirikala, W. Zhao, and A. E. Willner, Opt. Lett. **39**, 1605 (2014).
10. E. Flood, W. H. Guo, D. Reid, M. Lynch, A. L. Bradley, L. P. Barry, and J. F. Donegan, Opt. Express **18**, 3618 (2010).
11. A. J. Zilkie, C. Lin, P. G. Wigley, in *Optical Fiber Communication Conference*, (Optical Society of America, 2009), paper JThA12.
12. A. Annoni and F. Morichetti, J. Lightwave Technol. **31**, 1447 (2013).
13. J. Schröder, O. Brasier, T. D. Vo, M. A. F. Roelens, S. Frisken, and B. J. Eggleton, Opt. Express **18**, 22299 (2010).
14. L. Jia, J. Song, T.-Y. Liow, Q. Fang, M. Yu, G. Q. Lo, and D.-L. Kwong, Opt. Express **20**, 8512 (2012).
15. C. P. Lai, J.-Y. Yang, A. S. Garg, M. S. Wang, M. R. Chitgarha, A. E. Willner, and K. Bergman, Opt. Express **19**, 14871 (2011).
16. J. M. Oh, M. Brodsky, L. E. Nelson, G. Cadena, and M. D. Feuer, Opt. Lett. **33**, 2065 (2008).
17. A. Almaiman, M. R. Chitgarha, W. Daab, M. Ziyadi, A. Mohajerin-Ariaei, S. Khaleghi, M. Willner, V. Vusirikala, W. Zhao, D. Kilper, L. Paraschis, A. Ahsan, M. Wang, K. Bergman, M. Tur, J. D. Touch, and A. E. Willner, in *Optical Fiber Communication Conference*, (Optical Society of America, 2014), paper W2A.30.
18. R. Schmogrow, B. Nebendahl, M. Winter, A. Josten, D. Hillerkuss, S. Koenig, J. Meyer, M. Dreschmann, M. Huebner, C. Koos, J. Becker, W. Freude, and J. Leuthold, IEEE Photon. Technol. Lett. **24**, 61 (2012).
19. H. Kawakami, E. Yoshida and Y. Miyamoto, Electron. Lett. **46**, 430 (2010).
20. H. Kawakami, T. Kobayashi, M. Yoshida, T. Kataoka and Y. Miyamoto, Opt. Express **22**, 28163 (2014).
21. M. Seimetz, *High-Order Modulation for Optical Fiber Transmission* (Springer, 2009).

References

1. D. C. Kilper, R. Bach, D. J. Blumenthal, D. Einstein, T. Landolsi, L. Ostar, M. Preiss, and A. E. Willner, "Optical Performance Monitoring," Journal of Lightwave Technology **22**, 294-304 (2004).
2. Zhongqi Pan, Changyuan Yu, and Alan E. Willner, "Optical performance monitoring for the next generation optical communication networks," Optical Fiber Technology **16**, 20-45 (2010).
3. J. H. Lee, H. Y. Choi, S. K. Shin, and Y. C. Chung, "A Review of the Polarization-Nulling Technique for Monitoring Optical-Signal-to-Noise Ratio in Dynamic WDM Networks," Journal of Lightwave Technology **24**, 4162-4171 (2006).
4. David J. Ives, Benn C. Thomsen, Robert Maher, and Seb J. Savory, "Estimating OSNR of equalised QPSK signals," Optics Express **19**, B661-B666 (2011).
5. Jonathan C. Li, Trevor B. Anderson, and Trefor J. Morgan, "Transponder Dependence Issues in Asynchronous Delay-Tap Monitoring," IEEE Photonics Technology Letters **23**, 983-985 (2011).
6. Donghe Zhao, Lixia Xi, Xianfeng Tang, Wenbo Zhang, Yaojun Qiao, and Xiaoguang Zhang, "Periodic Training Sequence Aided In-Band OSNR Monitoring in Digital Coherent Receiver," IEEE Photonics Journal **6**, 7902009 (2014).
7. X. Liu, Y.-H. Kao, S. Chandrasekhar, I. Kang, S. Cabot, and L. L. Buhl, "OSNR Monitoring Method for OOK and DPSK Based on Optical Delay Interferometer," IEEE Photonics Technology Letters **19**, 1172-1174 (2007).
8. Yannick Keith Lizé, Jeng-Yuan Yang, Louis Christen, Xiaoxia Wu, Scott Nuccio, Teng Wu, Alan E. Willner, Raman Kashyap, and François Séguin, "Simultaneous and Independent Monitoring of OSNR, Chromatic and Polarization Mode Dispersion for NRZ-OOK, DPSK and Duobinary," in *Optical Fiber Communication Conference and Exposition and The National Fiber Optic Engineers Conference*, OSA Technical Digest Series (CD) (Optical Society of America, 2007), paper OThN2.
9. Mohammad Reza Chitgarha, Salman Khaleghi, Wajih Daab, Ahmed Almaiman, Morteza Ziyadi, Amirhossein Mohajerin-Ariaei, Devora Rogawski, Moshe Tur, Joseph D. Touch, Vijay Vusirikala, Wendy Zhao, and Alan E. Willner, "Demonstration of in-service wavelength division multiplexing optical-signal-to-noise ratio performance monitoring and operating guidelines for coherent data channels with different modulation formats and various baud rates," Optics Letters **39**, 1605-1608 (2014).
10. E. Flood, W. H. Guo, D. Reid, M. Lynch, A. L. Bradley, L. P. Barry, and J. F. Donegan, "In-band OSNR monitoring using a pair of Michelson fiber interferometers," Optics Express **18**, 3618-3625 (2010).
11. Aaron J. Zilkie, Christopher Lin, Peter G. Wigley, "Effect of Neighboring Channels in OSNR Monitoring With Fractional-Bit-Delay Interferometers," in *Optical Fiber Communication Conference and National Fiber Optic Engineers Conference*, OSA Technical Digest (CD) (Optical Society of America, 2009), paper JThA12.
12. A. Annoni and F. Morichetti, "Enhancing the Sensitivity of Interferometer Based In-Band OSNR Monitoring by Narrow Band Filtering," Journal of Lightwave Technology **31**, 1447-1453 (2013).
13. Jochen Schröder, Owen Brasier, Trung D. Vo, Michaël A. F. Roelens, Steve Frisken, and Benjamin J. Eggleton, "Simultaneous multi-channel OSNR monitoring with a wavelength selective switch," Optics Express **18**, 22299-22304 (2010).
14. Lianxi Jia, Junfeng Song, Tsung-Yang Liow, Qing Fang, Mingbin Yu, G. Q. Lo, and Dim-Lee Kwong, "Integrated in-band optical signal-to-noise ratio monitor implemented on SOI platform," Optics Express **20**, 8512-8517 (2012).
15. Caroline P. Lai, Jeng-Yuan Yang, Ajay S. Garg, Michael S. Wang, Mohammad R. Chitgarha, Alan E. Willner, and Keren Bergman, "Experimental demonstration of packet-rate 10-Gb/s OOK OSNR monitoring for QoS-aware cross-layer packet protection," Optics Express **19**, 14871-14882 (2011).
16. J. M. Oh, M. Brodsky, L. E. Nelson, G. Cadena, and M. D. Feuer, "Interferometric optical signal-to-noise ratio measurements of telecom signals with degraded extinction ratio," Optics Letters **33**, 2065-2067 (2008).
17. A. Almaiman, M. R. Chitgarha, W. Daab, M. Ziyadi, A. Mohajerin-Ariaei, S. Khaleghi, M. Willner, V. Vusirikala, W. Zhao, D.Kilper, L. Paraschis, A. Ahsan, M. Wang, K. Bergman, M. Tur, J. D. Touch, and A. E. Willner, "Experimental Demonstration of Robustness and Accuracy of an MZI-based OSNR Monitor under Transmitter Drift and Reconfigurable Networking Conditions for Pol-Muxed 25- Gbaud QPSK and 16-QAM Channels," in *Optical Fiber Communication*, OSA Technical Digest (online) (Optical Society of America, 2014), paper W2A.30.
18. Rene Schmogrow, Bernd Nebendahl, Marcus Winter, Arne Josten, David Hillerkuss, Swen Koenig, Joachim Meyer, Michael Dreschmann, Michael Huebner, Christian Koos, Juergen Becker, Wolfgang Freude, and Juerg Leuthold, "Error Vector Magnitude as a Performance Measure for Advanced Modulation Formats," IEEE Photonics Technology Letters **24**, 61-63 (2012).
19. H. Kawakami, E. Yoshida and Y. Miyamoto, "Asymmetric dithering technique for bias condition monitoring in optical QPSK modulator," Electronics Letters **46**, 430-431 (2010).
20. Hiroto Kawakami, Takayuki Kobayashi, Mitsuteru Yoshida, Tomoyoshi Kataoka and Yutaka Miyamoto, "Auto bias control and bias hold circuit for IQ-modulator in flexible optical QAM transmitter with Nyquist filtering," Optics Express **22**, 28163-28168 (2014).
21. Matthias Seimetz, *High-Order Modulation for Optical Fiber Transmission* (Springer, 2009).